Viscosities of Methane and Propane at Low Temperatures and High Pressures

E. T. S. HUANG, G. W. SWIFT, and FRED KURATA

University of Kansas, Lawrence, Kansas

The viscosities of methane and propane were determined at pressures to 5,000 lb./sq. in. abs. over a temperature range from —170° to 0°C. and —100° to 0°C., respectively, and the densities of propane were measured at pressures to 5,000 lb./sq. in. abs. over the temperature range from —100° to 0°C. Reproducibility of the viscosity data was about ± 1.2% and for the most part agreement with literature values was within ± 2%. The estimated accuracy of the density measurement was ± 0.5%. The data reported were well correlated in terms of residual viscosity vs. density.

Although the viscosity of methane in the superambient temperature region has been investigated extensively (*1* to *3*, *5*, *8*, *9*, *11*, *19*, *21*), there are relatively few data reported at low temperatures. Pavlovich and Timrot (*18*) reported the viscosity of methane at temperatures to —161°C. and pressures to 2,940 lb./sq.in.abs. Ross and Brown (*19*) measured the viscosity of methane at temperatures to —50°C. and pressures to 10,000 lb./sq.in. gauge. Barua et al. (*2*) made measurements on methane viscosity at temperatures to —50°C. and at pressures to 2,500 lb./sq.in. gauge. Swift et al. (*28*) extended the liquid viscosity range for methane from the atmospheric pressure range reported by Rossini et al. (*20*) to the critical point.

The data coverage for propane is similar to that of methane. At superambient temperatures a number of investigators have reported propane viscosities (*1*, *3*, *6*, *9*, *11*, *22*, *25* to *28*) while only the data of Swift (*27*), which extend to —65°C. and those of Rossini et al. (*20*), which extend from —40°C. to the freezing point, are available at subambient temperature.

In this study, the data for methane and propane in the low temperature range have been extended to pressures of 5,000 lb./sq.in.abs. The temperature range covered for methane was —170° to 0°C. and for propane, —100° to 0°C. These data, together with those cited above, give reasonably complete coverage of the viscosity-pressure-temperature domain for methane and propane in the liquid, gas, and dense fluid regions.

APPARATUS AND MATERIALS

The apparatus used in this investigation is similar to that reported by Swift et al. (*28*) but incorporates certain modifications which extend the upper operating pressure limit to 12,000 lb./sq.in.abs. To date the apparatus has not been operated at pressures above 5,000 lb./sq.in.abs. because of the limitations of pressure measuring equipment available.

The viscometer used is of the falling cylinder type (see Figure 1). An assembly consisting of a right circular cylinder of aluminum (*A*) with protrusions (*E*) for making electrical contact and pins (*H*) for aligning the cylinder concentrically within the vertically positioned precision bore tube (*B*) made of AISI 316 stainless steel is used to make the viscosity measurements. Cylinder (*A*) is raised to the top of tube (*B*) by the action of a magnet [mounted externally to tube (*B*)] on the two mild steel rods (*G*) imbedded in cylinder (*A*). As upper protrusion (*E*) on cylinder (*A*) comes into contact with electrical lead (*O*) of the top electrical lead assembly (*C*), cylinder (*A*) is disengaged from the magnetic field and falls through the fluid confined in tube (*B*). The breaking of the electrical contact between upper protrusion (*E*) on cylinder (*A*) and electrical lead (*O*) of the top electrical lead assembly (*C*) initiates a time count on a time interval meter. The making of the electrical contact between lower protrusion (*E*) on cylinder (*A*) and electrical lead (*O*) of the bottom electrical lead assembly (*D*) terminates the time count. The tube (*B*) forms the ground side of the circuit in both initiation and termination steps of the time count. The electrical leads (*O*) are insulated from tube (*B*) as shown in Figure 1. Electrical lead (*O*) makes a nonconducting, unsupported-area pressure seal with shoulder (*Q*) of plug (*M*) via Mylar gasket (*N*). Insulator (*L*) spaces electrical lead (*O*) through the port in plug (*M*) to prevent shortcircuiting. Washer (*K*) and lock nut (*J*) hold the assembly together and are tightened to effect the initial (zero pressure) seal between electrical lead (*O*) and plug (*M*).

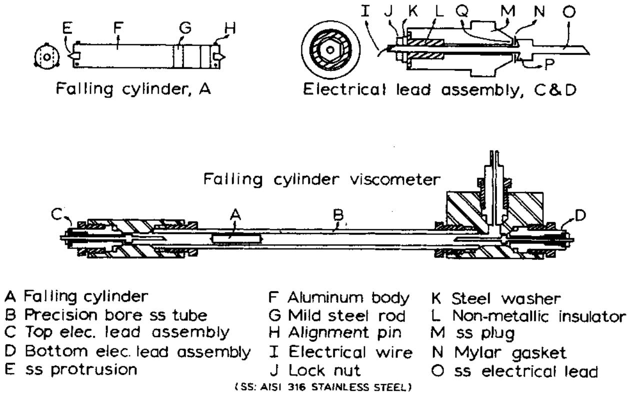

Fig. 1. Diagram of viscometer assembly.

The viscometer is housed in a controlled temperature bath which is a modified version of the one described by Sinor (*24*). The heat transfer medium for the bath is gaseous nitrogen at a pressure slightly above atmospheric pressure. The nitrogen is circulated by a high-speed centrifugal blower powered by an air motor. Liquid nitrogen at atmospheric pressure is used as coolant; the vaporized nitrogen is injected directly into the bath as heat transfer medium makeup. Coolant control is effected by controlling the back-pressure on the bath. An electrical resistance wire heater provides the amount of heat necessary to offset the liquid nitrogen vaporization load at a preset temperature level. The resistance setting on the bridge of a platinum resistance thermometer-Mueller bridge-d.c. null detector system sets the temperature level in the bath. A signal from the d.c. null detector reflecting the difference between thermometer temperature and set-point temperature is fed to a solid state temperature control device which in turn proportionally controls the voltage drop across the resistance wire heater.

Temperature measurement and control at all temperature levels employed in this investigation were within ± 0.01°C. The platinum resistance thermometer used for this purpose was calibrated against a similar instrument, which in turn had been calibrated directly by the National Bureau of Standards. Temperature differences between thermometer and various points on the viscometer were less than 0.1°C. as measured by thermocouples whose reference junctions were mounted on the sensing element of the thermometer.

Pressure measurements were made with a 5,000 lb./sq.in.abs. Bourdon tube gauge which had a maximum uncertainty of ± 5 lb./sq.in. The pressure gauge was calibrated against a pressure balance accurate to ± 1 lb./sq.in. Time of fall data was reproducible to ± 0.2% at 98% confidence and was measured with a Beckman Model 5230R-4 time interval meter.

The density measurements reported in this investigation were determined with a precision bore, high-pressure burette which displaced measured volumes of fluid into the viscometer at a constant temperature and pressure. The data of Kvalnes and Gaddy (*14*) and of Sage and Lacey (*23*) were used to convert the volumes of fluid transferred to masses of fluid transferred. The accuracy of the density data reported in this study is estimated to be ± 0.5%.

Phillips pure grade (99 mole % minimum) methane and instrument grade (99.5 mole % minimum) propane were used in this investigation. These materials were introduced into the apparatus via tubes filled with ascarite and phosphorus pentoxide to remove trace quantities of water and carbon dioxide. Analyses of the two materials by F & M Model 720 chromatograph with a silica gel column are as follows:

	Mole %				
	Methane	Ethane	Propane	*n* — Butane	Nitrogen
Pure grade methane	99.31	0.15	0.01	---	0.53
Instr. grade propane	trace	---	99.97	0.03	trace

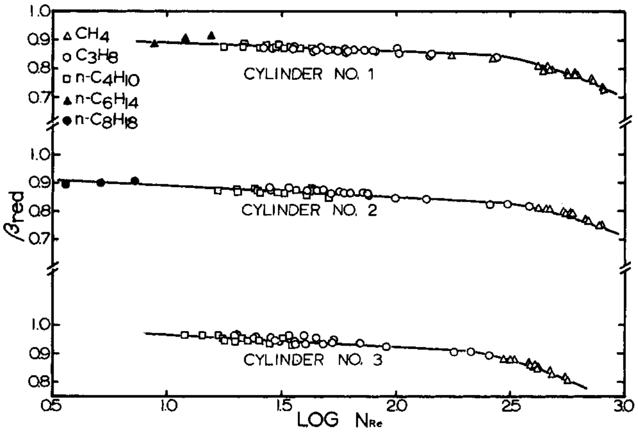

Fig. 2. Viscometer calibration plot.

CALIBRATION OF THE VISCOMETER

The theory of the falling cylinder viscometer and the method for correlating experimental calibration data in terms of the theory have been discussed in detail (*15*, *16*). The calibration data for the viscometer used in this investigation are expressed in the form

$$\beta_{\text{red}} = \beta_{\text{exp}}/\beta_{\text{calc}} = f(N_{Re}) = f(D_e s\rho/\theta\mu) \qquad (1)$$

where β_{exp}, the viscometer constant determined experimentally by measuring times of fall for calibrating fluids, whose densities and viscosities are known, at various temperatures and pressures, is defined as

$$\beta_{\text{exp}} = \mu s/[(\sigma - \rho)\theta] \qquad (2)$$

β_{calc}, the viscometer constant derived theoretically in terms of the physical dimensions of the instrument, is defined as

$$\beta_{\text{calc}} = gD_e^2(1-\kappa^2)^4(1-\kappa)^2/\{32\kappa^6(1+\kappa^2) \\ [(1+\kappa^2)\ln(1/\kappa) - (1-\kappa^2)]\} \qquad (3)$$

and D_e, the equivalent diameter for the annular gap between the falling cylinder and the viscometer fall tube, follows from the definitions for the Reynolds number N_{Re}, the friction factor f [see Equation (6.1-1) of Bird et al. (*4*)], and $f = 16/N_{Re}$, and is expressed as

$$D_e = 2\kappa^4 D_t[(1+\kappa^2)\ln(1/\kappa) \\ - (1-\kappa^2)]/[(1-\kappa)(1-\kappa^2)^2] \qquad (4)$$

The physical dimensions of the viscometer, s, D_c, D_t and $\kappa = D_c/D_t$, are expressed as functions of temperature and pressure (*16*) in the relationships above so that all calibration data, expressed in terms of Equation (1), are independent of temperature and pressure effects; that is, β_{red} is a function only of the flow regime prevailing in the viscometer. β_{red} can approach unity in the limit as s/θ approaches zero and is less than unity for finite values of s/θ because entrance and exit effects, alignment pin friction, etc., are not taken into effect in the theoretical development of β_{calc}. The effect of body acceleration to terminal velocity in the viscometer has been shown to be negligible at all Reynolds numbers encountered in this study (*13*).

The fluids for calibration were selected so as to encompass the range of Reynolds numbers anticipated in

TABLE 1. CALIBRATION RESULTS

Cyl. No.	Cyl. dia., in.	$\log(N_{Re})tr$	A_0	A_1	% Error*	B_0	B_1	B_2	% Error†	$\log(N_{Re})_{\max}$‡
1	0.3077	2.446	0.9351	—0.03870	±0.61	0.3633	0.5441	—0.1427	±0.81	2.917
2	0.3078	2.488	0.9353	—0.04462	±0.85	—0.6431	1.2495	—0.2656	±0.83	2.904
3	0.3087	2.327	1.0207	—0.04888	±0.81	—0.3075	1.1564	—0.2730	±0.65	2.750

* † Percentage errors for Equations (5) and (6), respectively, are reported as average percentage errors of the data points from the regression curves.
‡ $\log(N_{Re})_{\max}$ is the largest $\log(N_{Re})$ encountered during the calibration.
The diameter of the viscometer tube was 0.3140 in. All dimensions of the apparatus were measured at 25°C.

the experimental investigation and to insure internal consistency of viscosity data insofar as possible. The fluids used (all Phillips 99 mole % minimum purity hydrocarbons) and the literature references for viscosity and density data were:

Fluid	Viscosity literature reference	Density literature reference
Methane	*2*	*14, 29*
Propane	*26*	*23*
n-Butane	*10*	*23*
n-Hexane and *n*-Octane	*20*	*20*

Three falling cylinders, each falling in the same viscometer tube, were calibrated, giving the results shown in Figure 2 and Table 1. The form of the functional relationship of Equation (1) was determined for each falling cylinder by regression analysis after observing that the data depicted in Figure 2 indicated transition points such that the form for regression at Reynolds numbers less than the transition value should be

$$\beta_{\rm red} = A_0 + A_1 \log(N_{Re}) \tag{5}$$

while at Reynolds numbers greater than the transition value, the regression form should be

$$\beta_{\rm red} = B_0 + B_1 \log(N_{Re}) + B_2 \,[\log(N_{Re})]^2 \tag{6}$$

To determine experimental viscosities, the calibration data are used as follows:

1. $\beta_{\rm calc}$, s, and D_e are computed for the temperature and pressure at which the experiment was conducted.
2. A trial value of μ is assumed and the Reynolds number is computed by using the experimentally determined fall time and the density at the temperature and pressure of the experiment (either from literature or experiment).
3. The appropriate regression relationship [Equation (5) or (6) for the falling cylinder used] is selected for the Reynolds number computed in step 2.
4. $\beta_{\rm exp}$ is computed from $\beta_{\rm calc}$, N_{Re}, and the appropriate regression relationship.
5. μ is computed from Equation (2) by using $\beta_{\rm exp}$, s, σ, and experimental data for θ and ρ.
6. This iterative procedure is continued until the assumed and computed values of μ agree to within an as-

Table 2. Recommended Viscosity Values for Liquid, Vapor, and Fluid Methane

Pressure, lb./sq. in. abs.	Temperature, °C. 0°	−25°	−50°	−60°	−70°	−80°
	Viscosity, micropoise					
14.7	101*	93*	85*	83	80	76
600	111*	103*	96*	92	90	94
800	115*	108*	104*	103	113	235
1,000	120	116	118	127	185	288
1,500	138	144	184	229	280	345
2,000	161	182	244	287	333	391
3,000	214	256	330	364	403	453
4,000	263	314	386	420	456	508
5,000	305	361	432	463	501	555
	−100°	−120°	−140°‡	−150°	−160°	−170°
14.7	71	64	58	55	52	1,440
Dew point†	75	66	58	55	52	50
Bubble point†	385	542	767	940	1,140	1,440
600	405	570	810	990	1,190	1,510
1,000	438	599	840	1,020	1,230	1,560
1,500	477	631	878	1,070	1,280	1,620
2,000	512	664	917	1,110	1,330	1,680
3,000	573	727	990	1,200	1,420	1,810
4,000	627	788	1,060	1,290	1,520	1,930
5,000	676	847	1,140	1,370	1,620	2,060

* Values obtained from the data of Barua et al. (*2*).
† Dew point and bubble point pressures are from the literature (*17*).
‡ The vapor phase viscosities at temperatures below −140°C. were extrapolated from the higher temperature data.

Table 3. Recommended Viscosity and Density Values for Liquid Propane

Pressure, lb./sq. in. abs.	Temperature, °C. 0° Viscosity Micropoise	0° density g./cc.	−20° Viscosity Micropoise	−20° density g./cc.	−40° Viscosity Micropoise	−40° density g./cc.
Bubble point*	1,260	0.528	1,550	0.554	1,940	0.578
1,000	1,380	0.540	1,670	0.564	2,070	0.587
2,000	1,490	0.551	1,800	0.573	2,210	0.594
3,000	1,600	0.561	1,910	0.582	2,340	0.602
4,000	1,710	0.569	2,030	0.589	2,470	0.608
5,000	1,810	0.576	2,150	0.595	2,600	0.613
	−60°		−80°		−100°	
Bubble point*	2.450	0.602	3,160	0.624	4,290	0.646
1,000	2,600	0.608	3,320	0.630	4,520	0.651
2,000	2,750	0.616	3,500	0.636	4,760	0.655
3,000	2,910	0.622	3,680	0.641	5,020	0.660
4,000	3,060	0.627	3,880	0.645	5,270	0.663
5,000	3,220	0.632	4,060	0.651	5,540	0.669

* Bubble point pressure values are from the literature (*12*).

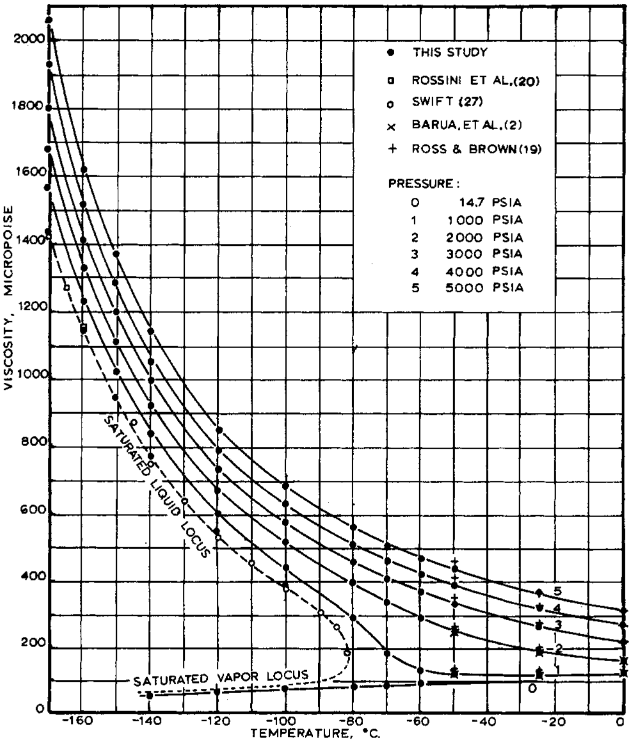

Fig. 3. Methane viscosity vs. temperature.

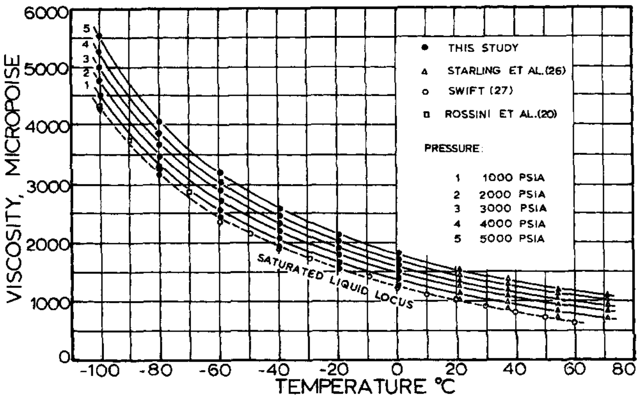

Fig. 4. Propane viscosity vs. temperature.

signed tolerance. This procedure is facilitated by using a digital computer.

In the experimental investigation, methane at most and propane at all of the temperatures and pressures covered were in the liquid or dense fluid states such that the Reynolds numbers were below the transition value. Certain of the low pressure-methane viscosity data were obtained at Reynolds numbers above the transition value. However, the highest log (N_{Re}) value encountered in this case was 2.992, so that only a modest extrapolation of the calibration was required.

EXPERIMENTAL RESULTS AND DISCUSSION

Experimental viscosity data were determined for methane at pressures to 5,000 lb./sq.in.abs. over the temperature range from −170° to 0°C. and experimental viscosity and density data were determined for propane at pressures to 5,000 lb./sq.in.abs. over the temperature range from −100° to 0°C. The viscosities for methane and propane were determined over the complete temperature and pressure ranges by using cylinder No. 1, while data were taken by using cylinders No. 2 and 3 for selected isotherms within the respective temperature ranges for methane and propane. The precision of the experimental viscosity measurements, determined by comparing the results obtained from the three cylinders for methane and propane, was ± 1.2% (*13*).

Table 2 presents the recommended values of viscosity for methane and Table 3 presents the recommended values of viscosity and density for propane. The viscosity data used to prepare these tables are those obtained from cylinder No. 1. For methane, the tabular information was extended to low pressures by using the viscosity data reported by Barua et al. (*2*) at 0°, −25°, and −50°C. The tabulated information presented was obtained from smoothed curves of viscosity (or density) as a function of pressure with temperature as a parameter. The recommended values presented in Tables 2 and 3 agree with the data of cylinder No. 1 to within ± 1%. The bubble and dew point viscosity values were obtained by extrapolation to the saturation pressures reported in the literature (*12, 17*). Vapor viscosities of methane at temperatures below −140°C. were obtained by extrapolation of higher temperature data, since no experimental vapor data were available at these temperatures.

The experimental data for methane and propane from cylinder No. 1 are presented in Figures 3 and 4, respectively, as graphs of viscosity vs. temperature with pressure as a parameter. These figures also compare the results of this study with those reported in the literature. For methane, the low-pressure liquid viscosities of this study agree with those reported by Rossini et al. (*20*) to within ± 1.4% but are consistently higher than those reported by Swift (*27*) by about 2.5%. Although Pavlovich and Timrot (*18*) reported liquid viscosities for methane, their data do not appear to be reliable since they are considerably higher than the values determined in this investigation and those reported by Rossini et al. and Swift (about 40% higher at −161°C.). In the higher temperature region for methane, the results of this study agree well with those of Barua et al. (*2*) which is to be expected, since those data were used in the calibration of the viscometer. The data reported by Ross and Brown (*19*) were consistently higher than those of this investigation by as much as 8.3%. The data obtained in the present study extrapolate smoothly to the superambient temperature values reported by Baron et al. (*1*), Carmichael et al. (*5*), and Giddings (*11*). For propane, the low-pressure liquid viscosities of this study agree with those reported by Swift (*27*) and Rossini et al. (*20*) to within ± 2.5% on the average, although the data of Swift were consistently lower by about 1.5%, and those of Rossini et al. were consistently higher at temperatures approaching the normal boiling point of propane by as much as 5.7%. Again, the data of this study extrapolate smoothly to the superambient temperature data reported by Starling et al. (*26*) which is to be expected, since these data were used in the viscometer calibration.

Figures 5 and 6 present the residual viscosity of methane and propane, respectively, as a function of density and compare the results of this study to those of other investigators. For propane, the atmospheric pressure viscosities used in computing residual viscosity were obtained by extrapolation of literature values (*6, 26*). The average deviation of methane data of this study from the curve presented in Figure 5 for densities greater than

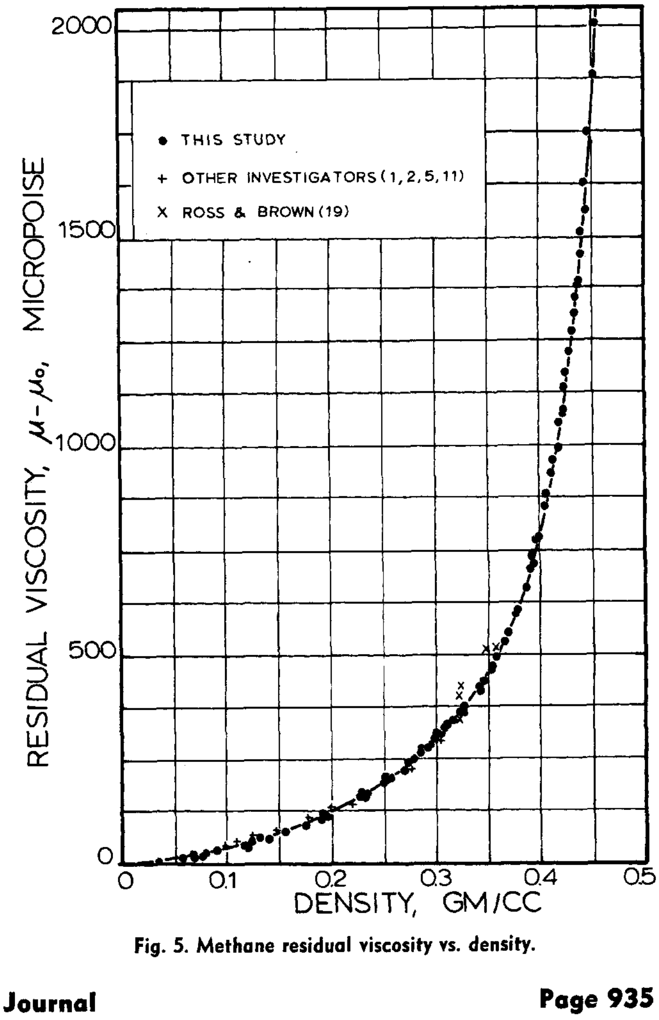

Fig. 5. Methane residual viscosity vs. density.

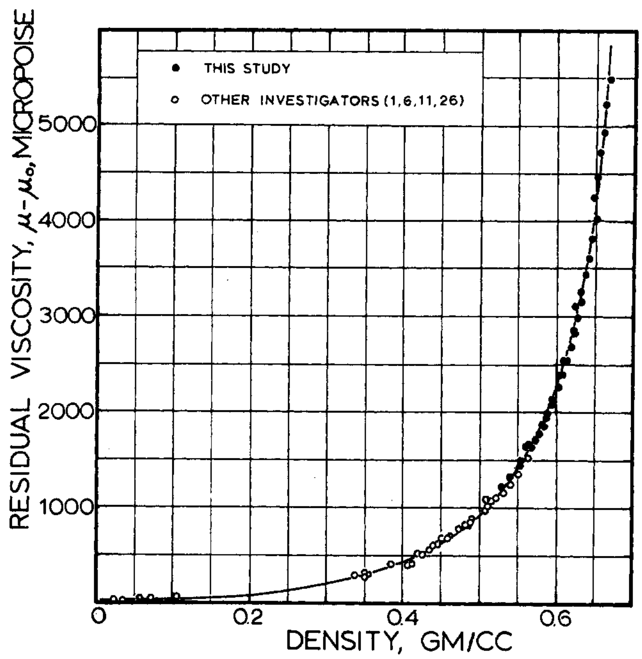

Fig. 6. Propane residual viscosity vs. density.

0.25 g./cc. is ± 1.0%, while for propane the average deviation from the curve presented in Figure 6 for all densities investigated is ± 1.5%.

CONCLUSIONS

A falling cylinder viscometer is described which is capable of measuring viscosities of light hydrocarbons in the gas, liquid, and dense fluid regions at pressures to 12,000 lb./sq.in.abs. over the temperature range from −170° to 100°C., while fluid densities are measured concurrently in the same instrument.

The viscosities of methane and propane were determined at pressures to 5,000 lb./sq.in.abs. over a temperature range from −170° to 0°C. and −100° to 0°C., respectively. The reproducibility of these data was on the average ± 1.2%, and agreement with literature values was for the most part within ± 2.0%. Densities of propane were determined at pressures to 5,000 lb./sq.in.abs. over the temperature range from −100° to 0°C. with an estimated accuracy of ± 0.5%.

The data of this study were used to extend the residual viscosity-density correlation well into the high density region. For methane, a smooth curve of the residual viscosity-density relationship represented the data of this study at densities greater than 0.25 g./cc. to within ± 1% on the average and for propane at all densities studied, the average deviation from the smooth curve was ± 1.5%.

ACKNOWLEDGMENT

Financial support for this work was furnished through the National Science Foundation Grant No. GP-386 and the University of Kansas Research Fund. Computer time was donated by the University of Kansas Computer Center and certain of the hydrocarbons used were furnished by the Phillips Petroleum Company.

NOTATION

A_0, A_1 = coefficients of Equation (5), dimensionless
B_0, B_1, B_2 = coefficients of Equation (6), dimensionless
D_c = O.D. of falling cylinder, cm.
D_e = equivalent diameter of viscometer [Equation (4)], cm.
D_t = I.D. of viscometer fall tube, cm.
f = friction factor, = $16/N_{Re}$, dimensionless
g = local acceleration of gravity, cm./sec.^{2}
N_{Re} = Reynolds number [Equation (1)] for viscometer, dimensionless
s = distance of fall in the viscometer, cm.

Greek Letters

β_{calc} = theoretical viscometer constant [Equation (3)], cc./sec.^{2}
β_{exp} = experimental viscometer constant [Equation (2)], cc./sec.^{2}
β_{red} = reduced viscometer constant [Equation (1)], dimensionless
θ = time of fall, cm./sec.
κ = D_c/D_t, dimensionless
μ = viscosity, g./(cm.)(sec.)
ρ = fluid density, g./cc.
σ = falling cylinder density, g./cc.

LITERATURE CITED

1. Baron, J. D., J. G. Roof, and F. W. Wells, *J. Chem. Eng. Data*, **4**, 283 (1959).
2. Barua, A. K., M. Afzal, G. P. Flynn, and J. Ross, *J. Chem. Phys.*, **41**, 374 (1964).
3. Bicher, L. B., and D. L. Katz, *Ind. Eng. Chem.*, **35**, 754 (1943).
4. Bird, R. B., W. E. Stewart, and E. N. Lightfoot, "Transport Phenomena," Wiley, New York (1960).
5. Carmichael, L. T., V. Berry, and B. H. Sage, *J. Chem. Engr. Data*, **10**, 57 (1965).
6. *Ibid.*, **9**, 411 (1964).
7. Carmichael, L. T., and B. H. Sage, *ibid.*, **8**, 612 (1963).
8. Carr, N. L., *Inst. Gas Technol. Res. Bull. 23* (1953).
9. Comings, E. W., R. J. Mayland, and R. S. Egly, *Univ. Illinois Engr. Expt. Sta. Bull. Serial 354* (1944).
10. Dolan, J. P., K. E. Starling, A. L. Lee, B. E. Eakin, and R. T. Ellington, *J. Chem. Eng. Data*, **8**, 396 (1963).
11. Giddings, J. G., Ph.D. thesis, Rice Univ., Houston, Tex. (1963).
12. Hanson, G. H., *Trans. Am. Inst. Chem. Engrs.*, **42**, 959 (1946).
13. Huang, E. T. S., Ph.D. thesis, Univ. Kansas, Lawrence (1966).
14. Kvalnes, H. M., and V. L. Gaddy, *J. Am. Chem. Soc.*, **53**, 394 (1931).
15. Lohrenz, John, and Fred Kurata, *A.I.Ch.E. J.*, **8**, 190 (1962).
16. Lohrenz, John, G. W. Swift, and Fred Kurata, *ibid.*, **6**, 547 (1960).
17. Matthews, C. S., and C. O. Hurd, *Trans. Am. Inst. Chem. Engrs.*, **42**, 55 (1946).
18. Pavlovich, N. V., and D. V. Timrot, *Teploenergetika*, **5**, No. 8, 61 (1958).
19. Ross, J. F., and G. M. Brown, *Ind. Eng. Chem.*, **49**, 2026 (1957).
20. Rossini, F. D., ed., "Selected Values of the Properties of Hydrocarbons and Related Compounds," Carnegie Press, Pittsburgh, Pa. (1958).
21. Sage, B. H., and W. N. Lacey, *Trans. Am. Inst. Mech. Engrs.*, **127**, 118 (1938).
22. ——————, *Ind. Eng. Chem.*, **30**, 829 (1938).
23. ——————, "Thermodynamic Properties of the Lighter Paraffin Hydrocarbons and Nitrogen," Am. Petrol. Inst., New York (1950).
24. Sinor, J. E., Ph.D. thesis, Univ. Kansas, Lawrence (1965).
25. Smith, A. S., and G. G. Brown, *Ind. Eng. Chem.*, **35**, 705 (1943).
26. Starling, K. E., B. E. Eakin, and R. T. Ellington, *A.I.Ch.E. J.*, **6**, 415 (1960).
27. Swift, G. W., Ph.D. thesis, Univ. Kansas, Lawrence (1959).
28. ———, John Lohrenz, and Fred Kurata, *A.I.Ch.E. J.*, **6**, 415 (1960).
29. van Itterbeek, A., O. Verbeke, and K. Staes, *Physica*, **29**, 742 (1963).

Manuscript received November 1, 1965; revision received March 9, 1966; paper accepted March 11, 1966. Paper presented at A.I.Ch.E. Dallas meeting.